



HAL
open science

Evidence for a disorder induced phase transition in the condensation of 4He in aerogels

Thierry Lambert, Florence Despetis, Laurent Puech, Pierre-Etienne Wolf

► **To cite this version:**

Thierry Lambert, Florence Despetis, Laurent Puech, Pierre-Etienne Wolf. Evidence for a disorder induced phase transition in the condensation of 4He in aerogels. 2006. hal-00021285v2

HAL Id: hal-00021285

<https://hal.science/hal-00021285v2>

Preprint submitted on 27 Dec 2006

HAL is a multi-disciplinary open access archive for the deposit and dissemination of scientific research documents, whether they are published or not. The documents may come from teaching and research institutions in France or abroad, or from public or private research centers.

L'archive ouverte pluridisciplinaire **HAL**, est destinée au dépôt et à la diffusion de documents scientifiques de niveau recherche, publiés ou non, émanant des établissements d'enseignement et de recherche français ou étrangers, des laboratoires publics ou privés.

Evidence for a disorder driven phase transition in the condensation of ^4He in aerogels

T. Lambert, F. Despetis (*), L. Puech and P.E. Wolf
Centre de Recherche sur les Très Basses Températures,
laboratoire associé à l'Université Joseph Fourier,
C.N.R.S., BP 166,
38042 Grenoble-Cedex 9, France
()Laboratoire des Colloïdes,*
Verres, et Nanomatériaux,
CNRS-Université Montpellier II Case Courrier 069,
34095 Montpellier-Cedex 5, France

(Dated: December 27, 2006)

Abstract

We report on thermodynamic and optical measurements of the condensation process of ^4He in two silica aerogels of same porosity 95%, but different microstructures resulting from different pH during synthesis. For a base-catalyzed aerogel, the temperature dependence of the shape of adsorption isotherms and of the morphology of the condensation process show evidence of a disorder driven transition, in agreement with recent theoretical predictions. This transition is not observed for a neutral-catalyzed aerogel, which we interpret as due to a larger disorder in this case.

PACS numbers: 64.60.-i, 64.70.Fx, 68.03.Cd, 67.70.+n

Condensation of fluids in mesoporous media, i.e. with pores sizes falling in the nm- μ m range, has long been the subject of extended research, both fundamental and applied [1]. From the point of view of statistical physics, this phenomenon offers an experimental realization of a phase transition in presence of disorder and confinement. From the practical point of view, it is widely used as a way to characterize the pore distribution. The most common case is that of sponge-like porous media, where the fluid is confined in well-defined cavities, either highly connected as, e.g., in Vycor glass, or with little or no connection, as in MCM41 silica. In the case where the dense phase of the fluid wets the substrate, one observes the progressive adsorption of a thin film at low vapor pressure, followed by a rather abrupt filling at a pressure of order, but smaller, than the saturated vapor pressure. This phenomenon is coined capillary condensation, being driven by the surface energy between the liquid and the vapor. In the classical picture, the condensation pressure depends on this surface energy and the pore size through the so-called Kelvin equation [1]. The process is hysteretic, emptying occurring at a lower pressure than filling. While this hysteresis is well understood at the level of the unique pore, its origin remains debated in the case of disordered porous media, with connected pores of different sizes [1, 2]. In particular, it has been recently shown by Kierlik *et al* [3] that it could result from the disordered nature of the porous media, rather than, as usually thought, of its geometry or topology ('pore-blocking'). In this new description, for a given pressure close to saturation, there exists a large number of metastable equilibrium states, the one being selected depending on the time history of the system, which gives rise to the observed hysteresis.

As such, this description should apply to porous media of very different topology, silica aerogels[4]. In these gels, the silica forms a complex arrangement of interconnected strands, resembling more a three-dimensional spider web than a sponge. Despite the positive curvature of the strands, which unfavors the film adsorption, aerogels fill below the saturated pressure, which, in a 'classical' picture, has been attributed to capillary condensation starting on the intersections between strands [5]. Experiments are however delicate to interpret as, due to their very low elastic modulus, the gels deform a lot upon adsorption of fluids with usual values of surface tension, such as nitrogen [6]. This leads to the idea of studying these gels using Helium, which has a much lower surface tension. Such an experiment, albeit differently motivated, was first performed by Wong and Chan, about 15 years ago [7]. Their results showed capillary condensation, but, quite surprisingly, at a well defined pressure

rather than on some range, as one would expect considering the wide distribution of scales in the silica aerogels. Together with specific heat experiments, this lead these authors to propose the existence of a genuine phase transition of helium inside aerogels, with a slightly depressed critical temperature with respect to the bulk case ($T_c = 5.195K$). However, latter experiments by other groups performed on similar aerogels (95% porosity, gelation process with basic pH), did not confirm this conclusion. The sorption isotherms are hysteretic, and condensation occurs over a finite range of pressures [8, 9, 10, 11]. Still, this range remains unexpectedly narrow, especially at low porosity [8, 12] or low temperature [11, 12].

Both facts are in agreement with theoretical work [4, 13] extending Kierlik *et al*'s description to a 95% porosity aerogel, numerically synthesized using diffusion limited cluster aggregation (DLCA), a process known to account for the structure factor of base-synthesized aerogels. These studies show a disorder-induced transition similar to that predicted by the Random Field Ising Model at zero temperature [14]. At small porosity (or large disorder), filling takes place by a succession of small, microscopic avalanches, where a limited number of sites switch from gas to liquid at each pressure. The maximal size of these avalanches increases with the porosity, up to some critical porosity (corresponding to some critical disorder), where it diverges. Above this critical porosity, which increases with increasing temperature, filling involves a macroscopic avalanche, associated with a jump in the average density, at some well defined pressure. This implies a change of shape, from smooth to sharp, of the hysteresis loop, when the porosity is increased at a constant temperature or, alternatively, when the temperature is decreased below some critical value, at a constant porosity. In magnetic systems, an equivalent change of the hysteresis loop has been observed in Co/CoO disordered films [15]. Although the observed evolution of shape with temperature is an appealing argument in favor of the Kierlik *et al* vision of the condensation in disordered porous media, other explanations could exist as well. The aim of this paper is to further investigate the adequacy of the proposed mechanism, and its possible dependence on the aerogel structure, using combined optical and thermodynamic measurements.

We used a one step process [16] to synthesize two aerogels of same porosity (95%), but different microstructures, by changing the pH from basic to neutral. Neutron [17] and X-ray [18] scattering experiments previously performed on similar samples reveal the sensitivity of the structure to the different kinetics of the sol-gel process in both cases. The size of the building silica units is larger for the base-catalyzed aerogel (B100, i.e. of density 100 kg/m^3)

than for the neutral aerogel (N102), whereas the correlation length is larger for N102 than for B100. This results in a fractal structure over a much larger range for N102 than for B100, and, accordingly, a wider distribution of pores sizes. The correlation lengths of our own samples were deduced from their structure factor $S(q)$ at zero q (as measured by light scattering) and their known porosities and fractal dimensions, using a theoretical expression of $S(0)$ which has been experimentally checked [19]. This gives values of order 10 nm for B100 and 20 nm for N102. Sorption isotherms were performed on both samples at a number of temperatures, and, at the same time, the way they scattered light was studied, so as to gain information on the distribution of helium inside the aerogels, both at the microscopic and macroscopic levels.

The experimental cell is a 4 mm thick copper block, traversed by a 20 mm diameter hole, and closed by two sapphire windows. Aerogels samples were sliced from 14 mm diameter cylinders. In the first experiment, we used a half disk of B100, about 2.7 mm thick. In the second experiment, we studied a 3.8 mm thick full disk of N102. The cell is mounted in a cryostat with 8 optical ports 45° apart, and is connected to the room temperature gas-handling system by two lines, one of which is used to fill or empty the cell through a regulated flowmeter, and the other is connected to a room temperature pressure sensor, with a resolution of 0.1 mbar. The flowrate is adjusted so that the stage of capillary condensation takes from 15 to 30 hours, which we checked to be long enough to get rate independent results.

The helium mass in the aerogel is obtained by integrating the flowrate over time, and correcting for dead volumes as discussed in ref.[11]. It is converted into a fraction Φ of dense phase ('liquid'), assuming that the vapor inside the aerogel has its bulk value and that the density of the dense phase is that measured for the fully filled aerogel[11].

Figure 1(a) shows the isotherms obtained at four temperatures below the bulk critical temperature T_c for the two aerogel samples. The general trends are in qualitative agreement with the usual picture of capillary condensation; the hysteresis loop gets narrower and closer to the bulk saturation pressure P_{sat} as the surface tension decreases with increasing temperature. Also, it is smoother, and closer to P_{sat} for N102, consistent with the wider distribution of pores extending up to larger sizes. Quantitatively, we measure the position of the adsorption isotherm by $\Delta P_{max} = P - P_{sat}$, at the point of largest slope of the adsorption branch. For a cylindrical pore of radius R , filling occurs at the stability limit

of the adsorbed film, which, for R much larger than the film thickness, is given by [20, 21] $\Delta P_{max} = \sigma/R \cdot \rho_V / (\rho_L - \rho_V)$, where σ is the helium surface tension, and ρ_L and ρ_V are the bulk liquid and vapor densities at saturation [22]. For a collection of independent pores, one expects ΔP_{max} to correspond to some typical value of the pores size. Although, *a priori*, aerogels cannot be so simply described, figure 2 shows that the equation above accounts for the temperature dependence of ΔP_{max} for N102 in the whole temperature range, and for B100 above 4.95 K, with characteristic ‘pores’ sizes $R \simeq 35$ nm and 20 nm. Both values are about twice the measured correlation lengths, a difference which is not surprising, considering the complex microstructure of the samples. However, this simple approach fails to describe the position of the pressure plateau for B100 at the two lower temperatures, which occurs at a smaller ΔP_{max} than expected. Furthermore, in such an approach, the small width of the corresponding isotherms would correspond to a much narrower distribution of pores sizes than that could be deduced from the isotherms at 4.95 K and above.

Optical measurements also show a markedly different behavior below 4.71 K, and above 4.95 K, respectively. We illuminate the aerogel by a thin (100 μ m wide), vertically polarized, He-Ne laser sheet under a 45° incidence with respect to its faces, and image it at 45°, 90°, and (for N102) 135° using CCD cameras. At any point of the intercept of the aerogel by the laser sheet, the brightness of the image is proportional to the intensity scattered by the aerogel in the direction of observation, and depends on the local strength and scale of the spatial fluctuations of the helium and silica densities. Figure 3 shows (a) images of B100 for increasing helium fractions along the previous isotherms, and (b) the scattered intensity by three selected spots in the images. Quantitative analysis of these curves show that, below $\Phi \approx 0.3$, the scattered intensity is that expected for a thin film of helium covering uniformly the silica strands, whereas, beyond this value, it becomes much larger, implying the formation of liquid clusters correlated over distances larger than the correlation length of the silica[11]. The striking fact is that, while this increase of the scattered intensity occurs uniformly over the sample for the two larger temperatures, for the two lower ones, it is only so for fractions less than about 0.5. Beyond, liquid progressively invades the aerogel, resulting in the growth of dark regions. Comparison of figures 1 and 3(b) shows that this invasion occurs along the vertical part of the isotherm. This could suggest that the bright and dark regions correspond to two coexisting phases at thermodynamic equilibrium. However, this is ruled out by the fact that the intensity scattered by the bright regions evolves with Φ , as

shown by figure 3(b) at 4.71 K. On the other hand, the observations exhibit the behavior expected for macroscopic avalanches ; at any given spot, the transition to the dark state occurs discontinuously, when this spot is swept by the boundary between the bright and the dark regions. This is consistent with the occurrence of a macroscopic (but local) avalanche from a partly filled to a fully filled state. In this scenario, the macroscopic morphology, which is identical for 4.47 K and 4.71 K, and for different rates of condensation as well, must originate in macroscopic, heterogeneities of the average density of silica, which make some regions favor slightly more the liquid. This will make the pressure at which the avalanche takes place to vary continuously in space, so that the transition should occur successively at different locations in the aerogel, in qualitative agreement with the observations.

In summary, for B100 at 4.71 K and below, the isotherms exhibit a nearly vertical portion, their position is anomalous, and a significant fraction of the condensation takes place in an heterogeneous way. These facts are consistent with the occurrence of a disorder induced transition for B100 between 4.95 K and 4.71 K. In contrast, for N102 at all temperatures, the isotherms are smooth, and the scattering is homogeneous, as shown in figure 4(a) : as a function of the condensed fraction Φ , the intensity scattered at 45° is the same along any vertical line of the picture, corresponding to a given depth, hence path length, inside the sample. There is a difference between points at different depths, but this (as well as the bump in the signal at $\Phi \approx 0.5$) can be explained by multiple scattering effects, which are stronger for N102 than for B100, due to the larger thickness and silica correlation length. Hence, no transition is observed for N102 in the temperature range where it is for B100. In the disorder induced transition scenario, this implies that the disorder does not only depend on porosity and is larger for N102 than for B100. We speculate that this is due to the wider distribution of pores sizes in this case. It would be interesting to see whether calculations performed on 95% aerogels numerically synthesized using the Diffusion Limited Aggregation algorithm appropriate for neutral aerogels would indeed confirm the absence of transition in this case.

Finally, as shown by figure 4 (b), the intensity scattered at 135° close to the entrance of the laser sheet, once corrected by the contrast factor $(\Delta n)^2$, where Δn is the difference in refractive index between the liquid and the vapor) behaves roughly the same, whatever the temperature. This suggests that, at a given Φ , the distribution of liquid does not depend on temperature. This is not the case for B100 below 4.95 K. As shown by figures 3(a) and

(b), the scattered intensity, at a given Φ , is smaller at 4.46 K than at 4.71 K, although the contrast is larger. This implies that the liquid must be distributed in smaller clusters. Here also, theoretical calculations would be needed in order to see whether such a temperature dependence follows from the disorder induced transition scenario.

In conclusion, our results provide a strong evidence for the occurrence of a disorder induced transition in the condensation of ^4He in base-catalyzed aerogels. Planned experiments using lighter aerogels should allow to check whether the transition moves to larger temperatures, as the theory would predict. Here again, the very low index of refraction of helium, which allows quantitative single scattering measurements to be performed over a much wider range of conditions than for any other simple fluid, will be a unique advantage. This ability to perform optical studies in transparent porous media could be used to study other problems as well, such as the origin of the hysteresis between adsorption and desorption.

We acknowledge T. Herman, J. Beamish, F. Detcheverry, E. Kierlik, M.L. Rosinberg, and J. Phalippou for useful suggestions or discussions.

-
- [1] For a review, see L. D. Gelb *et al.*, Rep. Prog. Phys. **62**, 1573 (1999).
 - [2] D. Wallacher *et al.*, Phys. Rev. Lett. **92**, 185701 (2004), and references therein.
 - [3] E. Kierlik *et al.*, Phys. Rev. Lett. **87**, 055701 (2001).
 - [4] F. Detcheverry, E. Kierlik, M. L. Rosinberg, and G. Tarjus, Phys. Rev. E. **68**, 061504 (2003).
 - [5] G. W. Scherer, J. Colloid Interf. Sci. **202**, 399 (1998).
 - [6] G. Reichenauer and G. W. Scherer, J. Non-Cryst. Solids **285**, 167 (2001).
 - [7] A. P. Y. Wong and M. H.W. Chan, Phys. Rev. Lett. **65**, 2567 (1990).
 - [8] D. J. Tulimieri, J. Yoon, and M. H. W. Chan, Phys. Rev. Lett. **82**, 121 (1999).
 - [9] J. Beamish and T. Herman, Physica B **340**, 329 (2003); J. Low Temp. Phys. **134**, 339 (2004).
 - [10] C. Gabay, P.E. Wolf, and L. Puech, Physica B **284**, 97 (2000); C. Gabay, F. Despetis, P.E. Wolf, and L. Puech, J. Low Temp. Phys. **121**, 585 (2000).
 - [11] T. Lambert, C. Gabay, L. Puech, and P.E. Wolf, J. Low Temp. Phys. **134**, 293 (2004); T. Lambert, Ph.D. thesis, Université Joseph Fourier, Grenoble I (2004).
 - [12] T. Herman, J. Day, and J. Beamish, Phys. Rev. B **72**, 184202 (2005).
 - [13] F. Detcheverry, E. Kierlik, M. L. Rosinberg, and G. Tarjus, Langmuir **20**, 8006 (2004); Phys.

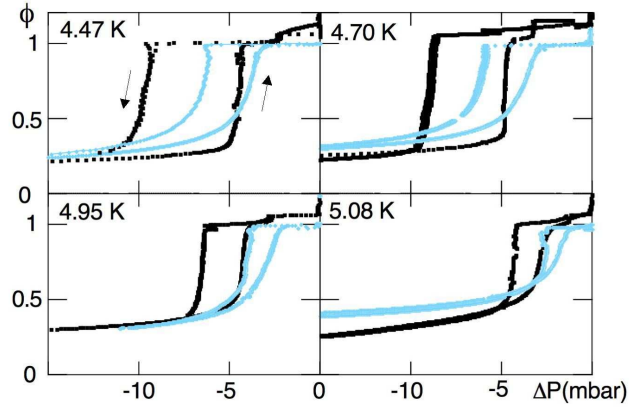


FIG. 1: (a) Isotherms at four temperatures, 4.47, 4.71, 4.96 and 5.08 K, for two aerogels of porosity 95%, B100 (black) and N102 (grey). The liquid fraction Φ in aerogel is plotted versus $\Delta P = P - P_{sat}$; for B100, there is a clear change of shape with temperature.

Rev. E **72**, 051506 (2005).

- [14] J. P. Sethna, K. Dahmen, S. Kartha, J. A. Krumhansl, B. W. Roberts, and J. D. Shore, Phys. Rev. Lett. **70**, 3347 (1993); O. Perkovic, K. Dahnen, and J. P. Sethna, Phys. Rev. B **59**, 6106 (1999).
- [15] A. Berger, A. Inomata, J. S. Jiang, J. E. Pearson, and S. D. Bader, Phys. Rev. Lett. **85**, 4176 (2000).
- [16] see e.g. J. Phalippou, T. Woignier, F. Despetis, S. Etienne-Calas, *Handbook of Sol Gel Science and Technology, Processing Characterization and Applications*, Kluwer Academic Publishers, Boston, 2005), Vol.1, p. 599.
- [17] R. Vacher, T. Woignier, J. Pelous, Phys. Rev. B **37**, 6500 (1988).
- [18] J. Wang, J. Shen, B. Zhou and X. Wu, Nanostruct. Mater. **7**, 699 (1996).
- [19] B. J. Frisken, F. Ferri, and D. S. Cannell, Phys. Rev. E **51**, 5922 (1995).
- [20] D. H. Everett and J.M. Haynes, J. Colloid Interf. Sci. **38**, 125 (1972).
- [21] W. F. Saam and M.W. Cole, Phys. Rev. B **11**, 1086 (1975).
- [22] This ΔP_{max} is half the value given by the Kelvin equation, which corresponds to the equilibrium of an hemispherical meniscus in the pore.

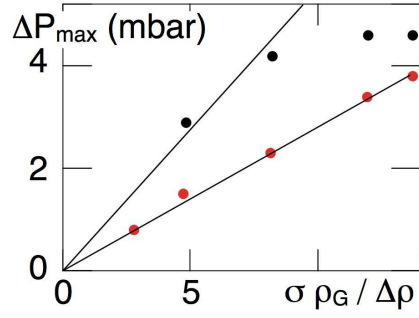


FIG. 2: Position ΔP_{max} of the point of maximal slope in the adsorption branch versus the temperature dependent ratio $\sigma\rho_V/(\rho_L - \rho_V)$. The straight lines correspond to pore diameters (see text) of 18 and 36 nm.

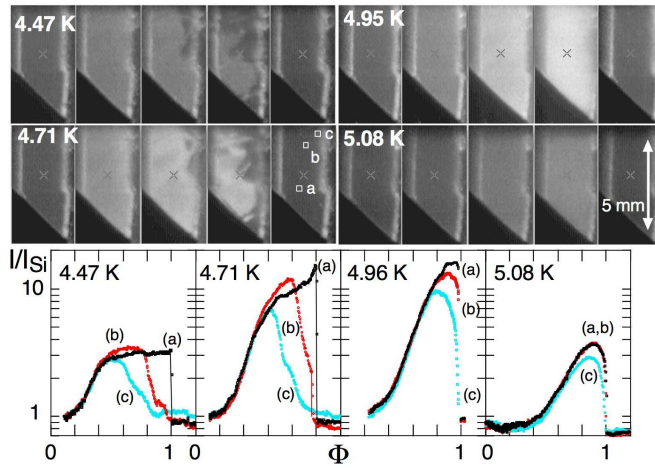


FIG. 3: Images of B100 observed at 45° from the incident laser sheet for helium fractions of 0.1, 0.5, 0.7, 0.9, and 1.0. The curves give the scattered intensity, referred to the empty aerogel situation, for the three regions labelled (a), (b), (c).

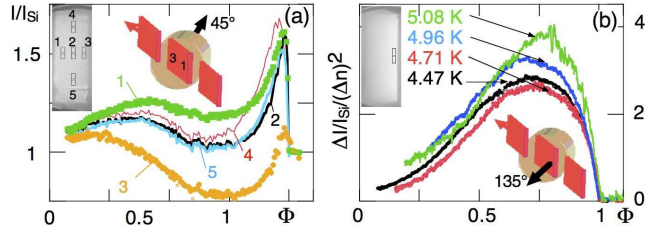


FIG. 4: Intensity scattered by N102 as a function of the condensed fraction Φ : (a) at 4.47 K and 45° . The signal, normalized by the silica contribution, corresponds to five regions at three different depths inside the aerogel disk. Differences between curves for different depths (and path lengths) are consistent with multiple scattering effects combined with an homogeneous distribution of the liquid clusters within the sample, in contrast to B100 at the same temperature; (b) at 135° , close to the entrance of the laser sheet. The silica contribution I_{Si} has been subtracted, and the result normalized by I_{Si} and the optical contrast squared. The signal is similar at all temperatures, suggesting that the spatial organization of the liquid only depends on Φ , not on temperature.